applied sciences

MDPI

Article

Wind Vulnerability of Flexible Outdoor Single-Post Billboards

Rolando Salgado-Estrada [1], Arturo Galván [2,*], Jatziri Y. Moreno-Martínez [2], Ernesto A. Elvira-Hernández [3], Franco Carpio [4], Agustín L. Herrera-May [5], Sergio A. Zamora Castro [1] and Israel E. Herrera-Díaz [6]

1. Faculty of Engineering of the Construction and the Habitat, Universidad Veracruzana, Calzada Adolfo Ruiz Cortines 455, Fracc. Costa Verde, C.P., Boca del Río 94294, Veracruz, Mexico; rosalgado@uv.mx (R.S.-E.); szamora@uv.mx (S.A.Z.C.)
2. Campus Celaya-Salvatierra, Universidad de Guanajuato, Av. Ing. Javier Barros Sierra 201, Col. Ejido de Santa María del Refugio, C.P., Celaya 38140, Guanajuato, Mexico; jatziri.moreno@ugto.mx
3. Facultad de Ingeniería Mecánica y Ciencias Navales, Universidad Veracruzana, Calzada Ruiz Cortines 455, Boca del Río 94294, Veracruz, Mexico; aelvirah@hotmail.com
4. Instituto de Ingeniería, Universidad Veracruzana, Av. Juan Pablo II S/N, Fracc. Costa Verde, C.P., Boca del Río 94294, Veracruz, Mexico; fcarpio@uv.mx
5. Micro and Nanotechnology Research Center, Universidad Veracruzana, Adolfo Ruíz Cortines 455, Boca del Río 94294, Veracruz, Mexico; leherrera@uv.mx
6. Campus Irapuato-Salamanca, Universidad de Guanajuato, Ex Hacienda El Copal km. 9, Carretera Irapuato-Silao, A.P. 311, C.P., Irapuato 36500, Guanajuato, Mexico; eherrera@ugto.mx

* Correspondence: arturo.galvan@ugto.mx; Tel.: +52-461-598-5922 (ext. 6304)

Abstract: Increased temperature due to global climate change is increasing the magnitude and frequency of extreme winds making billboard structures more vulnerable. This paper proposes a methodology to determine the structural safety of flexible outdoor single-post billboards. A CFD model of a flexible single-post billboard was performed as an example. Resultant wind forces were obtained for the previous model using different wind speeds. A mechanical numerical model of the billboard was realized, and this was subjected to the resultant wind forces. Internal forces for the most vulnerable places of the billboard were obtained for all different adopted wind speeds. Next, a reliability analysis of the billboard was performed considering several values for the bias factor and coefficient of variation for the internal forces caused by wind. Safety levels determined from the reliability analysis indicate that a billboard designed with a nominal wind speed of 180 km/h cannot achieve the target probability index of 3.2 for wind speed higher or equal to 200 km/h for any of the adopted probabilistic parameters. Significant differences in the found safety levels for the evaluated probability parameters indicate that billboard structures could undergo safety values below the target one with changes in the case where wind characteristics endanger this type of structure.

Keywords: flexible single-post billboards; wind engineering; wind loads; reliability analysis; CFD

Citation: Salgado-Estrada, R.; Galván, A.; Moreno-Martínez, J.Y.; Elvira-Hernández, E.A.; Carpio, F.; Herrera-May, A.L.; Zamora Castro, S.A.; Herrera-Díaz, I.E. Wind Vulnerability of Flexible Outdoor Single-Post Billboards. *Appl. Sci.* **2023**, *13*, 6197. https://doi.org/10.3390/app13106197

Academic Editor: Yingying Zhang

Received: 5 April 2023
Revised: 12 May 2023
Accepted: 16 May 2023
Published: 18 May 2023

1. Introduction

Since the end of the 20th century, the use of billboards has increased considerably because they are a means of outdoor advertising that can meet the sales and image expectations of advertisers, in addition, they are highly effective, productive, profitable and low cost. Increased temperature caused by global climate change increases the number of hurricanes and extreme wind events. This frequency and wind speed increase could make structures such as billboards more vulnerable.

These structures are built based on steel angles and tubular elements, many of them supported by a single column without redundancy capacity, and with a significant area in contact with the wind as can be seen in Figure 1.

In addition, many billboards have been built without complying with construction regulations and, on many occasions, do not consider the criteria established in the structural design codes and regulations of mentioned structures. Therefore, they are vulnerable to wind gusts caused by hurricanes, storms and other atmospheric events. Some authors have reported damage in this type of structure, for instance, Wang et al. [1], Wen and Xie [2], Warnitchai et al. [3] and Li et al. [4]. The lack of an adequate structural design in this type of structure can cause partial or total damage, causing material and human losses. The most vulnerable part of billboards is the supporting structure. Their typical failures are caused by exceeding the capacity of flexure-compression of the main tube, flexural capacity of the base plate and tensile capacity of the anchor rods. To detect these damages in advance, several techniques based on structural health monitoring (SHM) can be applied. This considers locating sensors to monitor the structural behavior by applying different damage detection methods. SHM has been applied successfully in structures such as wind turbines, which are similar to billboards [5]. One example of these typical failures is shown in Figure 2.

Figure 1. Typical single post billboards.

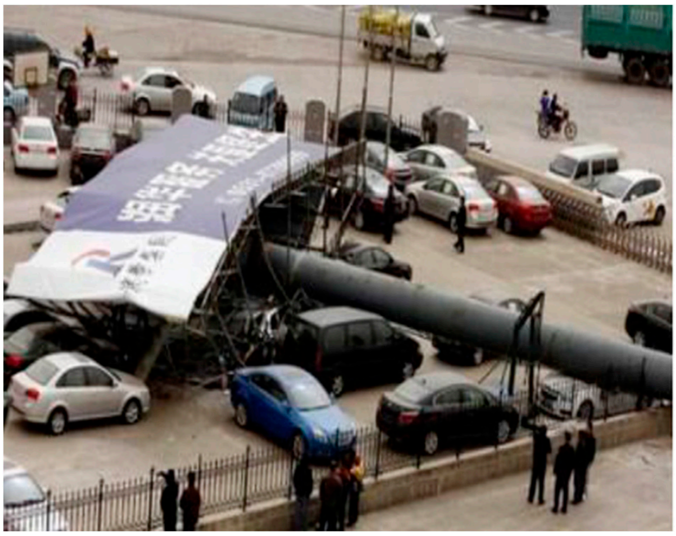

Figure 2. Typical failure in the support of single-post large billboards. Source [4].

Wind is an atmospheric phenomenon whose pressures on structures fluctuate. The magnitudes of the pressures depend on height, structural configuration, wind direction angle, also called angle of attack, wind turbulence and various other factors. Although these factors have been mostly included in the wind design manuals and codes, there are uncertainties in the structural response when there are flexible billboards that can have an important aeroelastic effect.

Despite the structural simplicity of billboards, their wind interaction is complex and depends on the size of the plate, total height, clear height and wind direction angle, among others. In professional practice, the billboard design is usually done by static methods, well-established in wind manuals and codes [6–8], underestimating the dynamic response when the billboard is flexible or is under high intensity wind gusts.

Due to the complexity of wind interaction with billboards, it has been necessary to carry out experimental tests. For instance, Letchford [9] studied the limit layer phenomena in rectangular signboards with different configurations by wind tunnel tests. He determined that important differences were found for drag forces for elevated panels. In this context, Li et al. [4] studied the wind dynamic effect in a tunnel test, of a single column, supported two-plate billboard structure. They determined the coefficients for a simplified wind design of this kind of structure. In this study a simplified procedure for the torsional analysis response was proposed. Paulotto et al. [10] researched the magnitudes of the pressure coefficients in rectangular plates by scale models tested in wind tunnels. Using scale model billboards, Warnitchai et al. [3] studied the effect of different wind direction angles in both the drag coefficient and the resultant torsional moment. Zuo et al. [11] performed experimental tests on rectangular signs in a wind tunnel. They determined that scale models with lateral holes are more prone to torsion. Moreover, they found that box signs would be over-designed according to current practice.

Experimental and full-scale tests need facilities, special sensors and equipment, which are not available in many cases. For this reason, computational fluid dynamics (CFD) has increased in importance to simulate the effect caused by wind in structures. In this way, Aly and Benson [12] performed CFD in standard, curve and porous signs. They found out that higher holes decrease drag forces compared with smaller ones.

To determine the safety level of these structures, a reliability analysis is necessary. Hoang [13] carried out a Monte Carlo simulation of rectangular signs considering as variables, wind speed, yield strength and column section properties. He determined that small changes in the wind speed led to larger differences in the safety level.

The objective of this research is to propose a methodology for determining the safety level of flexible single-post billboards subjected to the effects of wind. To achieve that, CFD analysis was performed in an adopted example of a billboard. Several wind speeds were chosen, and resultant forces were obtained and applied later in a finite element model of this structure. Structural reliability analyses were performed, and reliability indices were obtained for each wind speed, probabilistic parameters of wind effects and three limit state functions according to the most vulnerable locations in the structure were determined.

The content of this paper is organized as follows: the proposed methodology is presented in Section 2, where the theoretical background of reliability analysis is explained (Section 2.1) and descriptions of the structural and fluid models (Sections 2.2 and 2.3, respectively) are given. The structural behavior of the described models and its validation is shown in Section 3. Next, the reliability analyses for the evaluated limit state functions are carried out in Section 4 where the main results are discussed.

2. Methodology

A general methodology is proposed to be applied to any flexible single-post billboard for determining its safety level. According to Figure 3, the proposed methodology recommends, first, determining the cross-sectional dimensions of the structural elements according to wind [6] and structural steel code [7]. Next, gust loading factor (GLF) can be obtained for the adopted wind code. Later, CFD analysis is performed and drag forces are increased by the GLF. Using the forces that result from the CFD analysis, a linear elastic structural analysis is carried out. Internal forces are obtained in the most demanded part of the structure. In this case, it was determined in the base of the column, base plate and anchor rods. Wind speed and its corresponding effects are site dependent. These could suffer modifications when the number of acquired wind speeds increases. Therefore, it is proposed to carry out the analysis not only for the wind speed proposed by the wind code established for the billboard site, but also for an interval of wind speeds. Bias factor, λ, and coefficient of variation, COV, of wind speed are probabilistic parameters with high uncertainty. In consequence, an interval of these variables is also adopted. For any wind speed, λ and COV of wind speed effects, a reliability analysis is performed, providing the determination of the reliability index as a result. When all the variables are evaluated in the reliability analysis the vulnerability curves are obtained. Besides these procedures, it is recommended to perform a pushover analysis of the structure with the same load profile determined from the CFD analysis.

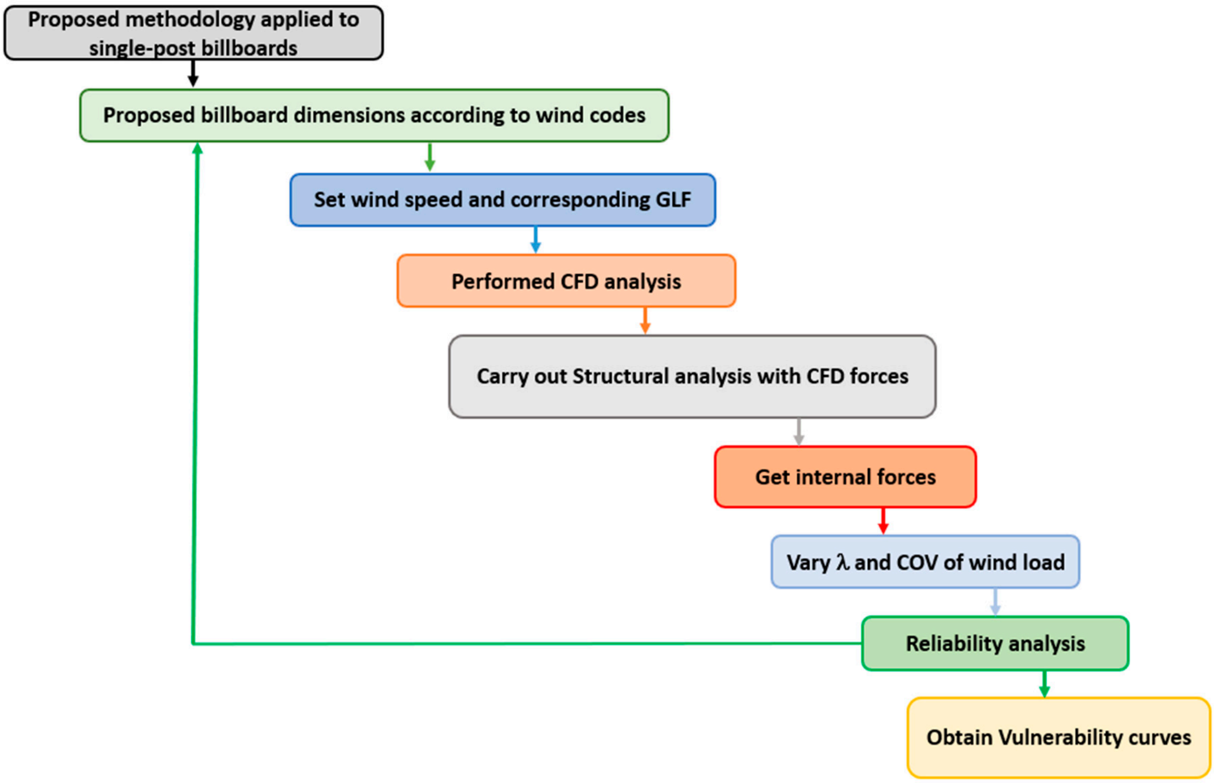

Figure 3. Flowchart of the proposed methodology.

2.1. Fundamentals of Structural Reliability

The safety level of structures can be determined, in most cases, by two different approaches. One of them is by using Monte Carlo simulations where, for the case study, the wind speed and cross-sectional dimensions are varied into certain intervals. Probabilistic distributions of the resistances and effect of the forces are obtained, and the probability of failure and reliability index of the structure could be determined. However, this approach is usually a time-consuming computation. The other approach consists of obtaining the main probabilistic values of the studied variables, namely, bias factor, λ, and coefficient of variation, COV. These values have been obtained in other studies for a variety of steel resistances and wind speed effects. Therefore, the last approach was adopted for performing the reliability analysis in this study.

For calculating the probability of failure and corresponding reliability index, a limit state G(X) function where X represents the random variables is defined. In this case, two random variables were considered, with loads indicated as S and resistances as R. In this way the failure region is when G(X) < 0 and the safety region is when G(X) > 0. Consequently, the probability of failure can be determined by Equation (1).

$$P_F = P[R - S < 0] = \int_{R-S<0} f_R(r)\, f_s(s)drds = \int_{-\infty}^{\infty} F_R(s)\, f_s(s)ds \tag{1}$$

where f_R and f_s are the probability density functions of the resistance and loads, respectively. F_R is the cumulative probability density function of the resistances.

Normally, probability of failure, P_F, gives values near zero and it is difficult to determine differences between two or more cases. In this case, it is better to use the reliability index, β, with common values in the interval between 0 and 10. A relationship between probability of failure and reliability index can be expressed by Equation (2).

$$\beta = \Phi^{-1}(1 - P_F) \tag{2}$$

where Φ^{-1} indicates the inverse of the normal standard probability distribution.

If loads and resistances are normal distributed variables, the reliability index is defined as the standard deviation times the distance between the mean value of the G(X) = R − S and the vertical axis, as it is shown in Figure 4. Frequently, loads and resistances are not normally distributed. Moreover, the algorithms to determine the safety level parameters depend on whether the limit state function is linear or not. Therefore, reliability analysis methods have been divided in two, namely: first-order reliability methods (FORM) for linear limit state functions and second-order reliability methods (SORM) for non-linear limit state functions. In this study, reliability analysis was performed with the help of the FERUM computer program [14], which employed the algorithms proposed by [15] and [16] for the FORM and SORM solutions, respectively.

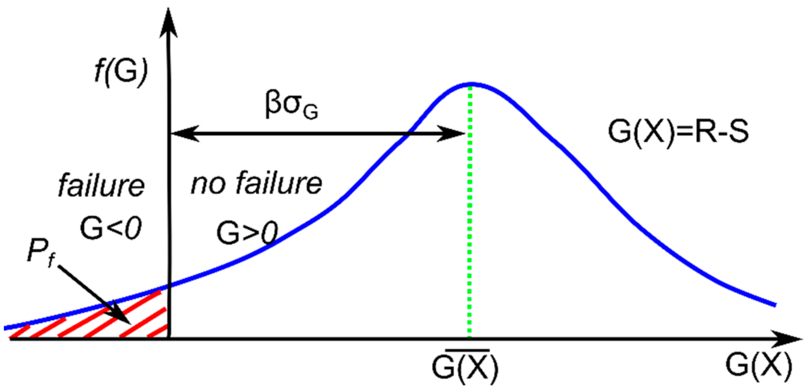

Figure 4. Probability of failure and reliability index for normal probability distribution variables. Adopted from Salgado et al. [17].

2.2. Description of Structural Model

The ANSYS commercial finite element package [18] was used to perform the structural and fluid computational models of one flexible single-post billboard under different wind speeds.

In the structural model (Figure 5), isoparametric solid elements identified as SOLID186 were used to simulate the panel, header, vertical steel pole support, base plate, angles, brackets, pedestal, nuts and anchor rods. This type of element is a higher order 3-D solid element with quadratic displacement behavior. The element is defined by 20 nodes having three degrees of freedom per node: translations in the nodal x, y and z directions. The element supports plasticity, hyperelasticity, creep, stress stiffening, large deflection and large strain capabilities. It also has mixed formulation capability for simulating deformations of nearly incompressible elastoplastic materials, and fully incompressible hyperelastic materials. SOLID187 element was also used for modeling zones of the single-post billboard where irregular meshes were required: some zones of vertical steel pole support, base plate and brackets. This solid is a higher order 3-D, 10-node element, which includes a quadratic displacement behavior, and this has three translational degrees of freedom at each node. To reduce the computational effort, the damage in the pedestal was ignored.

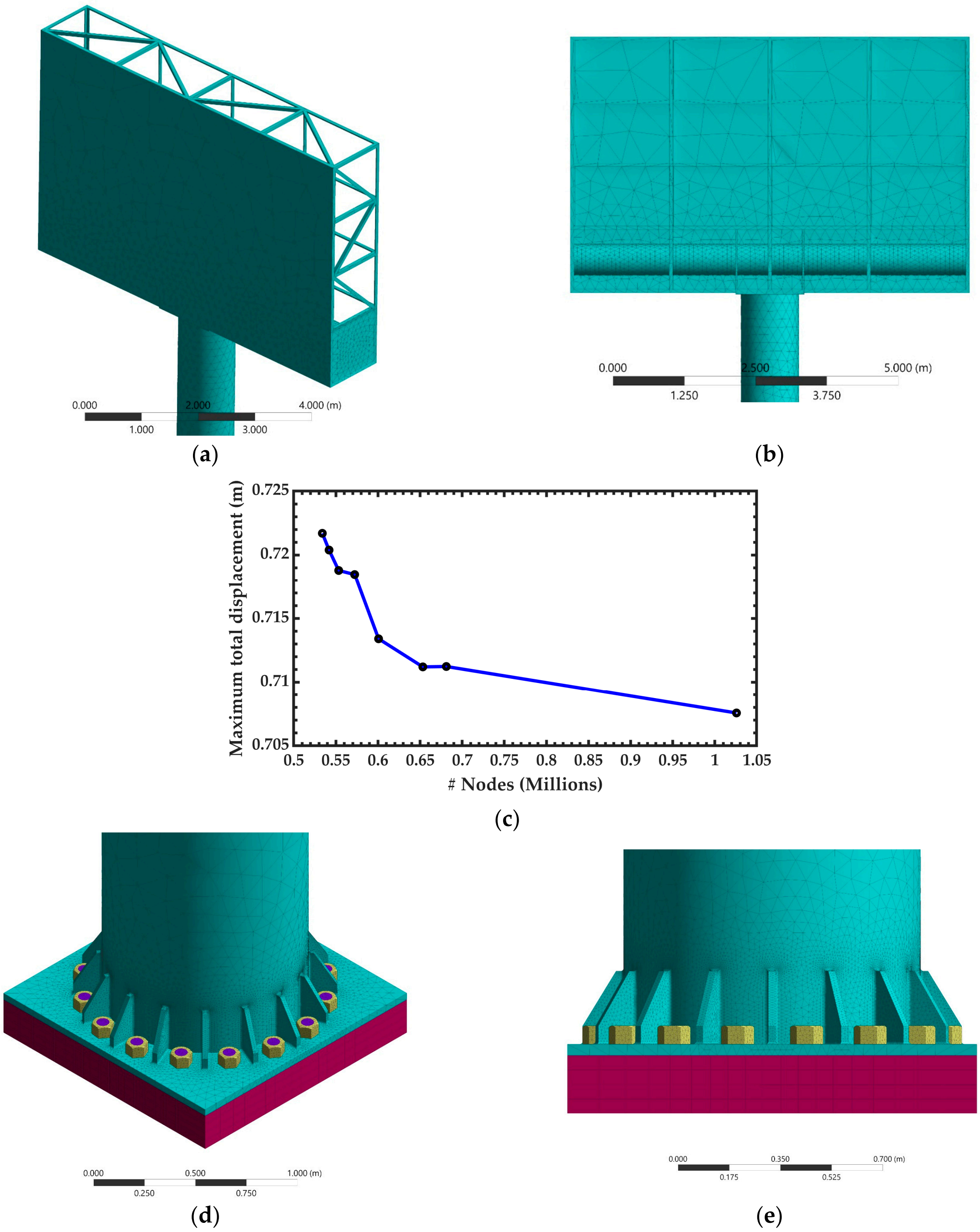

Figure 5. Three-dimensional nonlinear numerical model of a flexible single-post billboard, based on FEM using ANSYS [18]: (**a**) isometric view (panel, vertical steel pole support and angles); (**b**) back view including the header; (**c**) mesh independence study; (**d**) isometric view (vertical steel pole, brackets, pedestal, nuts and anchor rods); (**e**) lateral view (vertical steel pole, brackets, pedestal, nuts and anchor rods).

For static structural analysis, the joints between anchor rods and base plate and the joints between anchor rods and the pedestal were modeled by using contact elements (Figure 5), whilst modal analysis was not included in these types of the elements due to the nature of this analysis; any nonlinearities such as plasticity and contact elements are ignored. Contact elements used are identified in ANSYS as CONTA174 and TARGE170; with these types of elements it is possible to create discontinuous finite element models. Thus, these elements can be used to model the following characteristics:

- The sliding, closure or opening of joints is allowed.
- When the joint is closed, there are transmissions of compressive and shear stresses but not of tensile stresses.
- When the joint is opened, there is no transmission of stresses.
- The transmission of shear stresses is according to Coulomb's law.
- Changes in the geometry can be detected because of the relative movement of the elements that form the joint.

For the joints, sliding between surfaces was considered according to Coulomb's law by using one coefficient of friction (isotropic friction) of 0.44 [19]. A mesh independence study was performed by considering the maximum total displacement obtained from the billboard as a function of the number of nodes generated in each simulation, obtaining a variation of this maximum displacement of less than 2% (Figure 5c), concluding that with 572,316 nodes generating 325,205 elements an average mesh quality of 0.74 is achieved; consuming a computational effort of 30 min by a workstation using 10 cores and 40 GB of RAM. The mechanical and geometrical properties used in the structural model are depicted in Tables 1 and 2, respectively.

Table 1. Mechanical properties of materials used in the flexible single-post billboard.

Material	Parameter	Value	Unit
Structural steel	Poisson ratio ν	0.3	
	Elastic modulus E	200,000	MPa
	Shear modulus G	76,923	MPa
	Yielding stress f_y	360	MPa
	Ultimate stress f_u	460	MPa
Concrete	Poisson ratio ν	0.2	
	Elastic modulus E	22,000	MPa
	Shear modulus G	9166	MPa

Table 2. Geometrical properties used in the flexible single-post billboard.

Structural Element	Section	Dimensions
Post	Circular tube	D = 1016 mm t = 22.2 mm
Panel	Angles	LI 63.5 × 12.7 mm
Pedestal	Circular tube	D = 550 mm t = 19.1 mm
Base plate	Square plate	B = 1400 mm H = 1400 mm t = 44.5 mm
Brackets	Trapezoidal plate	Bs = 50 mm Bi = 150 mm H = 250 mm
Anchor rods	Cylindrical	D = 63.5 mm h = 300 mm
Nuts		D = 98.425 mm d = 50.8 mm h = 63.62 mm

Geometrical properties of the billboard were determined after several cycles of modification of its main structural elements comparing their resistances and corresponding internal forces calculated for the initial reference wind speed of 180 km/h. The structural steel design of the main structural elements included in Table 2 was performed using the ANSI/AISC 360-22 [20] steel design code.

Finally, contact elements identified as SURF154 were used in the static structural analysis to apply the pressure to the billboard. This element allows complex pressure loads.

2.3. Description of Fluid Model

Simulations to determine the pressures generated by the wind on the billboard were carried out using ANSYS CFX 16.2 commercial fluid dynamics software. In the fluid model, tetrahedral solid elements with 4 nodes identified as MESH200 were used to simulate the air volume used in computational fluid dynamics, CFD, analysis as depicted in Figure 6. This volume considered as a continuous flow of air was an ideal gas at 25 °C at a reference pressure of 1 atm and initial speeds in u, v and w of 0 km/h with a relative pressure of 0 Pa. The dimensions of the volume (80 m $\times$ 70 m $\times$ 318 m) guarantee the development of the fluid and avoid interference between the walls and the billboard. In the numerical model, the Z and X axes were parallel to the westerly and southerly wind directions, respectively.

The analysis was defined as steady-state isothermal using the shear stress transport (SST) turbulence model and the convergence criterion was defined as 1×10^{-4}. The three walls (top and sides) of the control volume were considered as free slip walls and the floor and all the surfaces that make up the geometry of the billboard and the area that the floor represents were considered as non-slip walls. To represent the variable wind speed at the domain input fluid, the power law was considered (Equation (3)).

$$u(y) = u_{ref}\left(\frac{y}{y_{ref}}\right)^{\alpha} \tag{3}$$

where u_{ref} and y_{ref} represent the reference speed and the reference height, respectively. To depict the most severe scenario, it was considered that the billboard was in a flat terrain without sudden topography changes and with obstacles less than 5 m height, and located in the Port of Veracruz, one of the cities with the most severe high intensity winds in Mexico. With these characteristics, the reference speed was set to 180 km/h, and the reference height was set to 10 m (CFE, [6]). For its part, the exponent α represents the stability of the atmosphere and for the study cases where the billboard is located near the coast, it was considered as 0.14 [21], whilst the volume outlet was considered as an outlet type and a relative pressure was assigned of 0 Pa.

To determine the vulnerability of the billboard, as an example, several wind reference speeds were adopted. Wind references along the Mexican coast can vary between 160 up to 220 km/h (CFE, [6]). Therefore, it is interesting to know how variations of the initial reference speed of 180 km/h causes changes in the safety levels of the structure. Here, wind reference speeds ranged from 160 to 220 km/h with increments of 10 km/h, to capture variations and trends of the safety levels, were considered for further analyses. Moreover, to take into account the dynamic interaction between the billboard structure and the wind, a gust load factor, GLF, was determined according to specifications given in CFE [6]. Table 3 indicates the wind reference speeds, and their gust loading factors (GLF) used in the computational fluid dynamics model. GLF indicates how many times the wind static response calculated with the CFD analysis needs to be incremented. From Table 3, it can be deduced that an important dynamic interaction, bigger than 2.0, is obtained for all wind reference speeds with higher values of GLF when wind reference speed increases.

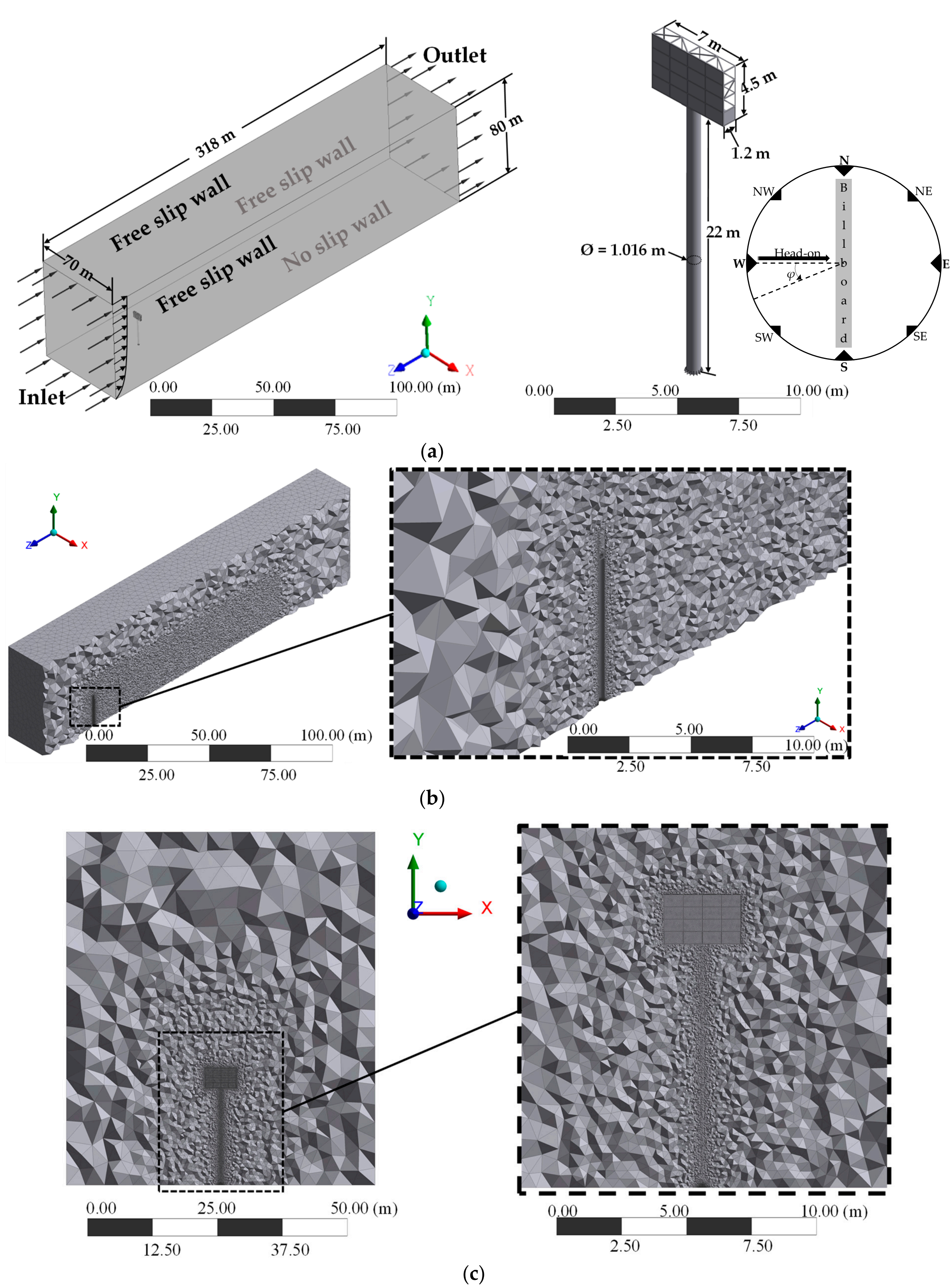

Figure 6. CFD model: (**a**) air volume, boundary conditions, geometry of the billboard and wind directions; (**b**) longitudinal section; (**c**) cross section.

Table 3. Wind reference speeds and GLF used in the analysis.

Wind Reference Speed (km/h)	Gust Loading Factor (GLF)
160	2.148
170	2.504
180	2.586
190	2.666
200	2.742
210	2.815
220	2.886

3. Wind Simulation Results and Validation with Experimental Results

CFD analysis applied to the conditions stablished in Section 2.3 for the wind reference speeds adopted here gave the following results:

As an example, the case of wind reference speed of 180 km/h was chosen. Similar results were obtained for other wind reference speeds. Its wind profile along the wind tunnel is depicted in Figure 7.

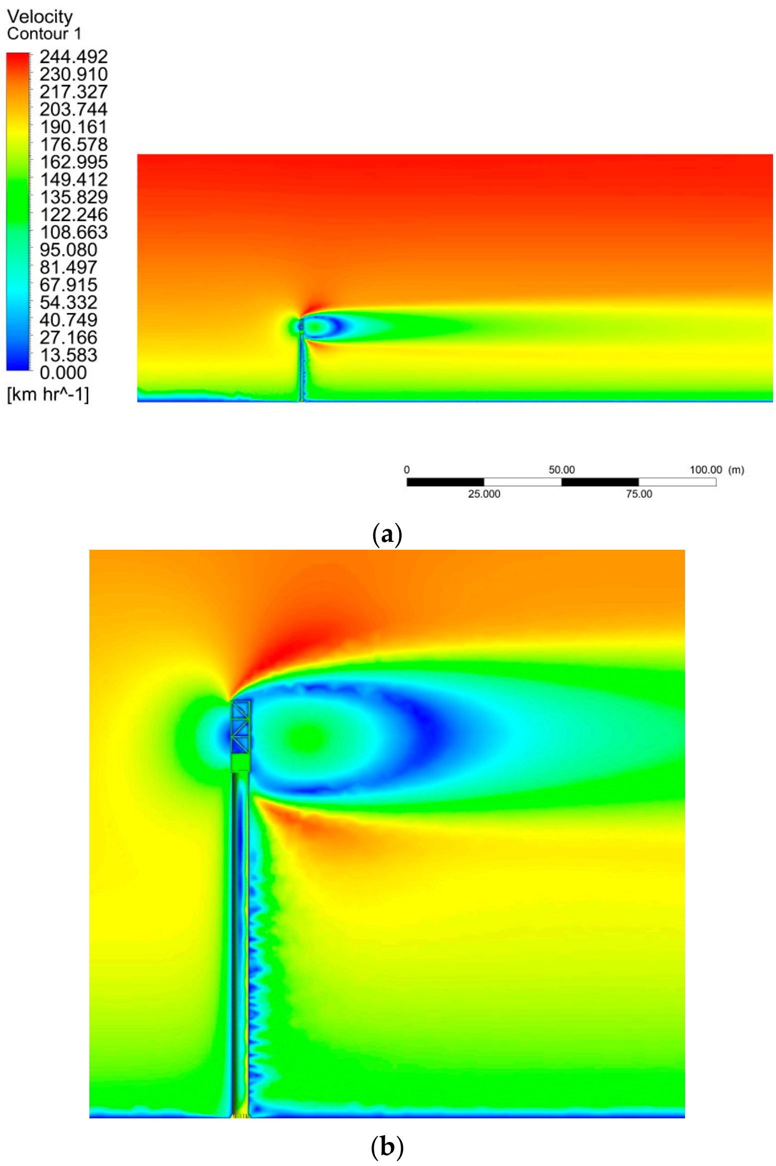

Figure 7. Longitudinal wind speed profile along wind tunnel: (**a**) Full view; (**b**) post billboard view.

From Figure 7 it can be deduced that the head-on wind speed profile before arriving the billboard indicates incremental speeds along its height between 100 near the bottom of the billboard to 190 km/h in the highest location of it.

The wind streamline deduced from Figure 7 is similar to those presented by Simiu and Yeo [22] for a square section, where the separation region in Figure 7 is at the top and bottom of the panel and the wake region is the place exactly back of the panel with a significant decrement of the wind speed.

Figure 8 shows the wind pressure for both evaluated directions. Pressure in the panel for the case of head-on direction is almost the same for all the panels, meanwhile the case of north eastbound direction has a variation of the wind pressure along the width of the panel as expected. This caused the torsional moment in this direction.

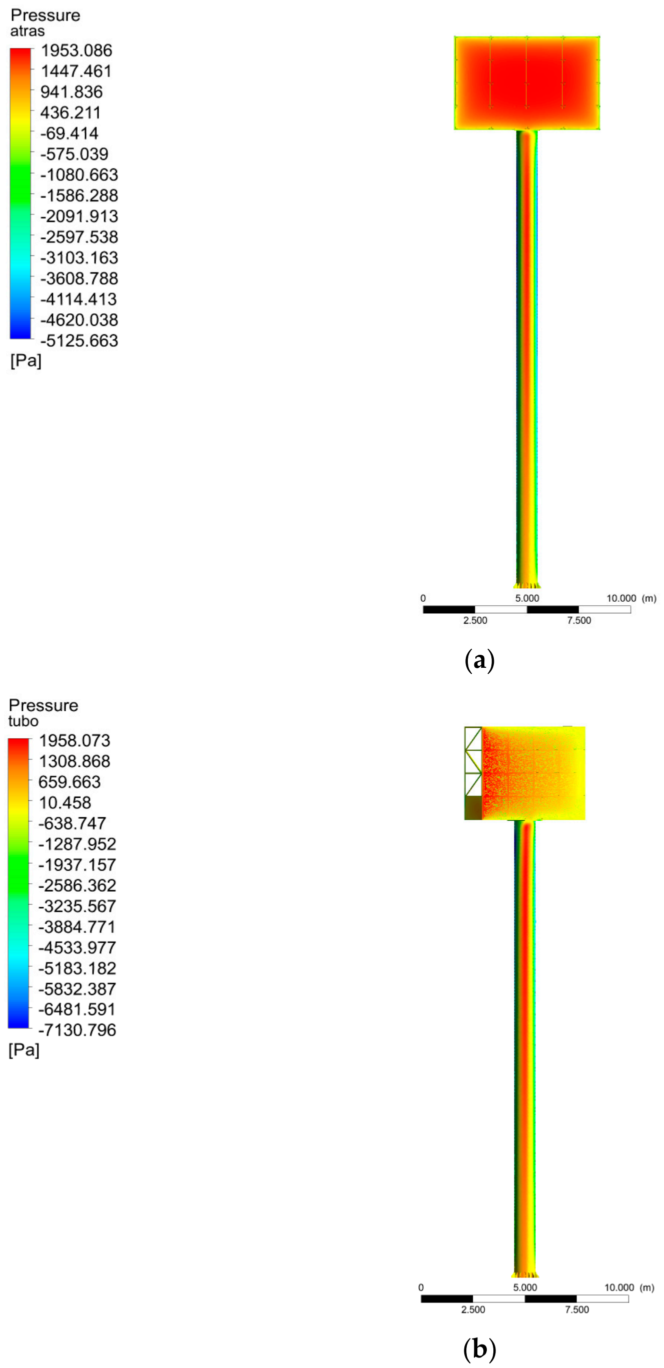

Figure 8. Wind pressure at 180 km/h: (**a**) head-on direction; (**b**) north eastbound direction.

Using data extracted from Figures 7 and 8, namely, the wind speeds and wind pressures, it was possible to determine the panel drag coefficient using Equation (4) and the required data shown in Tables 4 and 5 for the head-on and east northbound wind directions, respectively.

$$C_f = \frac{P_0}{1/2\rho V_D^2} \tag{4}$$

where P_0 is the panel wind pressure, ρ is the mass density specified here as 1.293 kg/m^3 of the wind and V_D is the mean value of the wind in the panel.

Table 4. Determination of drag coefficients from CFD analysis for head-on wind direction.

Wind Reference Speed (km/h)	Panel Pressure P_0 (MPa)	Wind Speed Middle Panel V_D (km/h)	Drag Coefficient C_f
160	1540	152	1.42
170	1740	158	1.48
180	1953	168	1.47
190	2178	177	1.48
200	2417	188	1.45
210	2668	197	1.46
220	2932	209	1.43

Table 5. Determination of drag coefficients from CFD analysis for north eastbound wind direction.

Wind Reference Speed (km/h)	Panel Pressure P_0 (MPa)	Wind Speed Middle Panel V_D (km/h)	Drag Coefficient C_f
160	1540	153	1.40
170	1740	160	1.45
180	1953	169	1.46
190	2178	178	1.47
200	2417	190	1.43
210	2668	199	1.44
220	2932	210	1.42

According to CFE [6], which presents drag coefficients based on experimental studies carried out by Letchford [9], drag coefficients for both wind directions for the evaluated billboard were determined at 1.45, which is in accordance with the results determined from Tables 4 and 5 with mean values of 1.46 and 1.44 for the cases of head-on and north eastbound directions, respectively.

Drag forces are validated by the internal forces obtained for the application of the wind loads in the structural numerical model of the billboard as shown in Section 4.1.

4. Structural Behavior

4.1. Linear Behavior

Modal analysis of single-post billboards was carried out to obtain their dynamic properties, achieving these can determine the gust loading factors (GLF) depicted in Table 3; these factors are used in the reference wind speeds applied to the numerical model. The first five mode shapes and their frequencies are depicted in Figure 9. Mode 1 moves in the northbound direction, parallel to the panel of the billboard (Figure 9a) with a period of 0.96 s, whilst mode 2 is associated with the head-on wind direction (Figure 9b) and it has a period of 0.95 s. Mode 3 is the torsional mode along the tube (Figure 9c), having a period of 0.16 s, whilst mode 4 (Figure 9d) and mode 5 (Figure 9e) are the second modes associated with transversal and longitudinal wind directions with periods of 0.14 s and 0.12 s, respectively. According to CFE [6], important dynamic effects can be obtained for structures with periods of wind direction from one second. Nevertheless, the GLF shown in Table 3 indicates high dynamic interaction with the wind-billboard even when the first mode, transversal to the panel, has a period of 0.95 s.

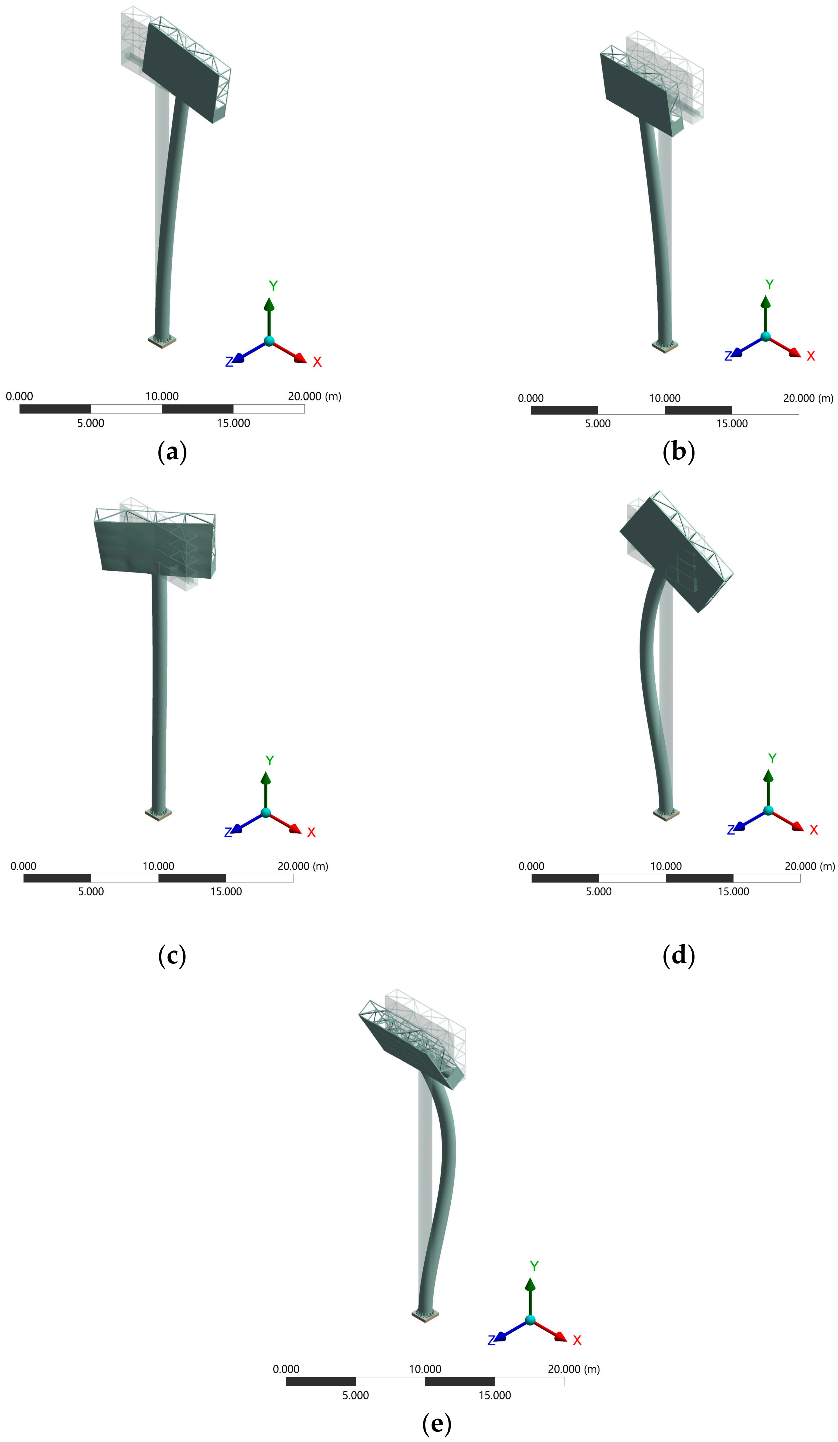

Figure 9. Mode shapes of single-post billboard: (**a**) mode 1, period = 0.96 s; (**b**) mode 2, period = 0.95 s; (**c**) mode 3, period = 0.16 s; (**d**) mode 4, period = 0.14 s; (**e**) mode 5, period = 0.12 s.

Using the wind forces determined from the CFD analysis for the different wind reference speed with their corresponding GLF, the total displacements were determined. As an example, Figure 10 depicts the wind reference speed of 180 km/h, obtaining maximum displacements of 0.86 and 0.77 m on the top of the panel by considering wind direction angles of head-on and north eastbound, respectively.

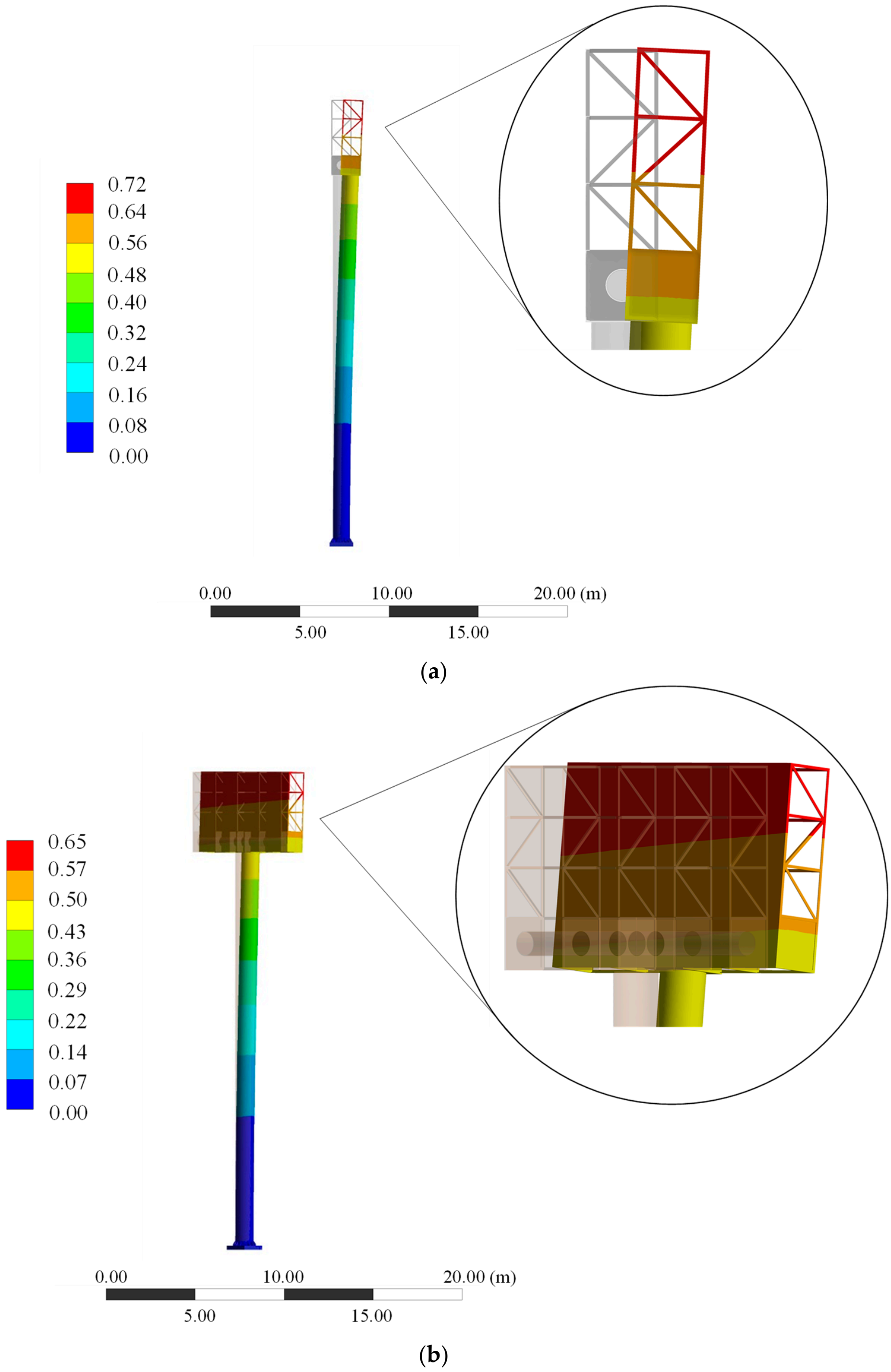

Figure 10. Displacements, in meters, obtained from the numerical model of single-post billboard under wind reference speed of 180 km/h: (**a**) wind direction angle at head-on; (**b**) wind direction angle of north eastbound.

The maximum displacements obtained for the seven wind reference speeds used in this study are depicted in Table 6. Maximum displacements of the billboard are bigger for head-on compared to north eastbound wind direction and differences become larger while increasing the wind speed, reaching a maximum of 13% difference for the wind reference speed of 220 km/h. The only exception was the case of 160 km/h. This behavior can be explained because wind force in the main tube for the north eastbound direction was projected in two orthogonal directions, therefore, its maximum displacements combined with those forces caused by wind in the panel are becoming smaller compared to the case of the head-on direction where the entire force of the wind is pushing the billboard in one direction. In the case of the lowest wind speed of 160 km/h, and maybe for lower wind speeds as well, the wind force in the panel dominates and considering that wind direction at north eastbound provokes a torsional effect on the billboard, its total displacements dominate in this range of wind speeds.

Table 6. Maximum displacements for different speeds.

Wind Reference Speed (km/h)	Maximum Displacements (m)	
	Head-On	North Eastbound
160	0.48	0.50
170	0.65	0.58
180	0.72	0.65
190	0.86	0.77
200	0.98	0.87
210	1.11	0.99
220	1.25	1.10

The internal forces calculated in the column base, the location of the maximum demand, have similar values for both wind directions, having the highest values for all evaluated wind speeds for the north eastbound wind direction, as can be shown for base shear force (Figure 11a), bending moment (Figure 11b) and torsional moment (Figure 11c). These internal forces are required for the design procedure and reliability analysis described later. For instance, base shear force and torsional moment are more relevant for the analyses of rods, meanwhile the bending moment is more relevant in the case of the column base and base plate analyses. It can be deduced that all internal forces increased by more than double comparing wind speeds at 160 km/h and 220 km/h. The torsional moment at head-on wind direction is negligible compared with the north eastbound wind direction, and no curve is shown in Figure 11c. Additionally, it can be noticed that internal forces increased in a parabolic way.

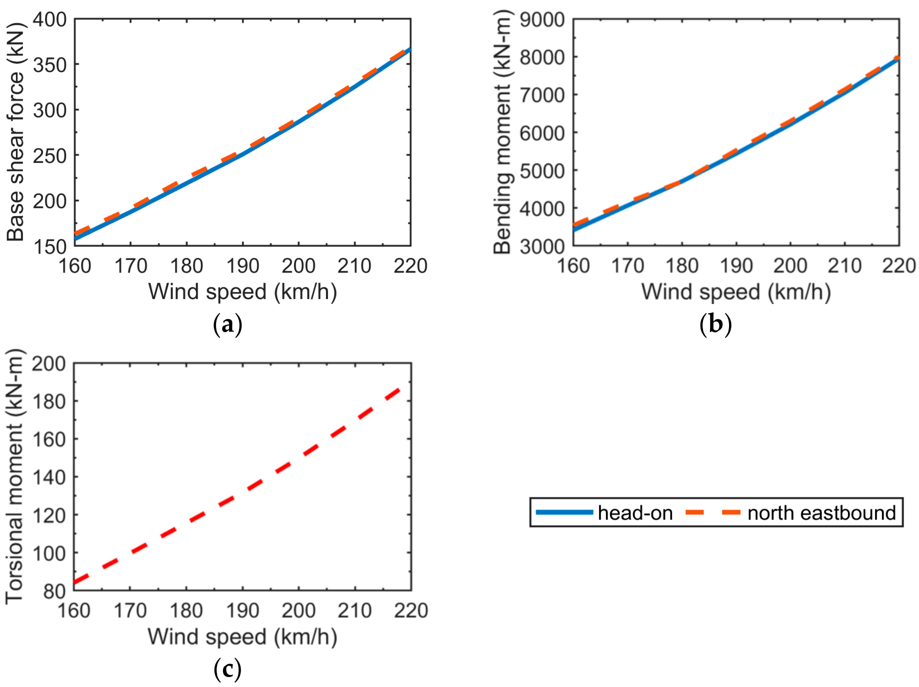

Figure 11. Internal forces determined in the column base of the billboard for head-on and north eastbound wind speed directions across the adopted wind speeds: (**a**) base shear force; (**b**) bending moment and (**c**) torsional moment.

To validate the wind forces obtained with the CFD numerical model, the internal forces evaluated in the column base depicted in Figure 9 were compared with those calculated using the CFE [6]. Internal forces differences of this comparison are shown in Table 7.

Table 7. Differences in the internal forces determined by CFD analysis and experimental results.

Wind Reference Speed (km/h)	Shear Force (%)		Bending Moment		Torsion (%)
	Head-On	North Eastbound	Head-On	North Eastbound	
160	0.10	11.17	1.71	9.78	2.47
170	0.31	11.25	3.61	10.09	3.77
180	0.50	13.80	2.17	7.59	1.72
190	0.69	11.33	4.20	10.17	3.07
200	0.95	11.58	4.44	1014	2.93
210	1.17	11.70	4.68	10.20	2.94
220	1.45	11.83	4.95	9.84	2.75
average	0.74	11.81	3.68	9.69	2.31

According to Table 7, shear force differences of the head-on wind direction have a mean of 0.74%, which indicates excellent correlation between numerical and experimental shear forces. In the case of north eastbound wind direction a mean of 11.81% was determined. This difference is considered due to the procedure for calculating the wind forces in the CFE procedure that does not take into account wind forces in the southbound direction, only in the head-on wind direction. In the case of the bending moment comparison related to the head-on wind direction, a different mean of 3.69% was found. This difference is attributed to the incremental bending moment caused by the deformed shape of the structural model after the application of the wind loads determined from the CFD analysis. The same reason is given for the moment differences for the north eastbound wind direction, but now a different mean of 9.69% is also caused by higher wind forces found in this direction in the CFD simulation as indicated in the shear force differences. Finally, torsional moment differences were determined. Here, for calculating the eccentricity of the wind force, the recommendation given by Letchford [9] of taking ten percent of the panel width was adopted. With this assumption, a torsional different mean of 2.31% was found. This difference is a good approximation of the CFD analysis compared with reported experimental results.

4.2. Structural Design

After calculating the internal forces for all adopted reference wind speeds, the resistant efficiencies of column, base plate and anchor rods were calculated according to the ANSI/AISC 360-22 [20] steel design code. The main purpose of that was to prove if billboard structural dimensions are adequate or not. Here, structural efficiency is defined as the ratio between the ultimate internal load, F_u, and the factored resistance, F_R. In Figure 12, the structural efficiencies in the above-mentioned structural elements of the billboard can be seen. The maximum allowable efficiency when internal loads are equal to resistances is shown with a gray dashed line. Below this line all the evaluated elements are considered adequate. From Figure 12 it can be deduced that anchor rods were overdesigned due to uncertainties about the ultimate tensile force having enough capacity to offer support with winds of up to 220 km/h. On the other hand, we have the case of the column base and base plate that have capacity to support wind speeds of up to 185 km/h and 190 km/h, respectively. Therefore, in the reliability analyses, only the base column and base plate were considered. It is important to emphasize that structural elements of billboard were designed for an initial wind reference of 180 km/h.

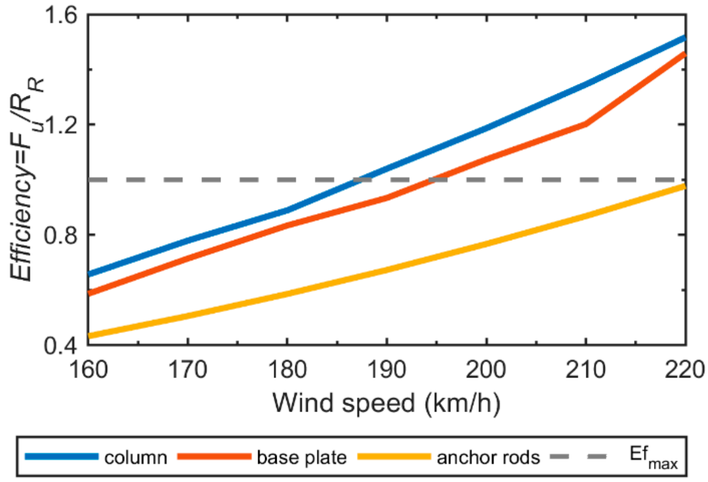

Figure 12. Structural efficiencies determined for the base column, base plate and anchor rods.

4.3. Non-Linear Behavior

A non-linear analysis of the flexible single-post billboard with the main purpose of determining its maximum structural capacity was performed. The flexure-compression failure was simulated with this non-linear analysis. Firstly, a bilinear elastic-plastic behavior, in both tension and compression, was defined for the main steel post tube. Its material properties were already established in Table 1. Additionally, a strain hardening slope of 1% was defined for the post-yielding curve. The stress–strain curve of the steel single-tube column is shown in Figure 13.

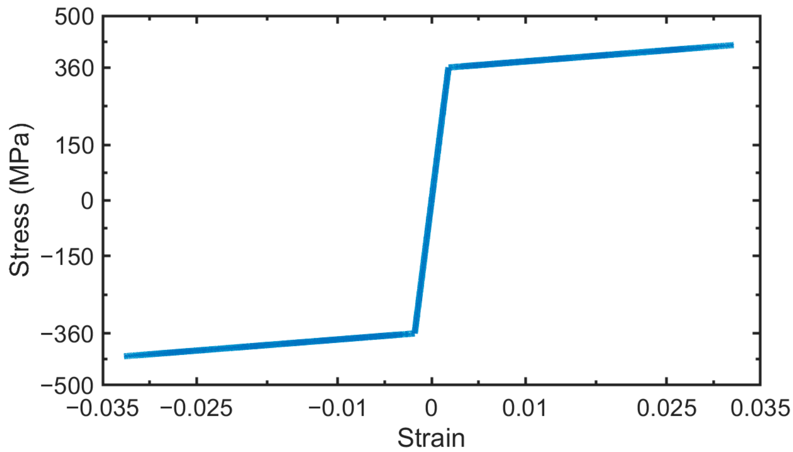

Figure 13. Stress–strain steel curve adopted for the non-linear analysis.

With the above-mentioned defined characteristics, a pushover analysis was performed. The same lateral load profile determined by the pseudo-static wind forces using the wind code (CFE [6]) was used here. Displacement control of the highest elevation node in the central panel was monitored for every millimeter. Base shear force was calculated every step until the monitored node reached 3600 mm, a value higher than the maximum displacement of 1250 mm reported in Table 8 for the highest wind speed of 220 km/h. The capacity curve, defined as the displacement of the monitored node versus base shear force, was finally obtained. It is also interesting determining the moment–curvature curve for the column base with the purpose of calculating the maximum moment capacity of the structure. Both the capacity and moment–curvature curves of the base column are shown in Figure 14a,b, respectively.

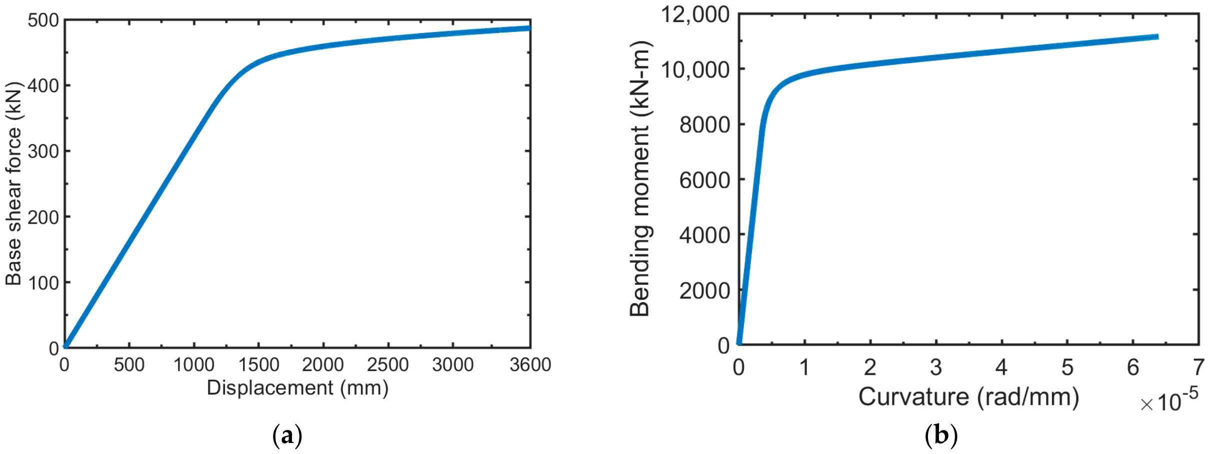

Figure 14. Pushover analysis results; (**a**) capacity curve and (**b**) moment–curvature curve in the base of the column.

From Figure 14a, it is possible to determine that the yield shear capacity of the billboard structure is around 400 kN, corresponding to a displacement of the top of the billboard of about 1500 mm. In the case of the yield bending moment determined from Figure 14b, a value of about 7000 kN-m was obtained with a yield curvature of about 0.5×10^{-5} rad/mm. If we compare these results with the maximum displacement, base shear force and bending moment given in Table 6 and Figure 11a,b, respectively, it is found that even for the highest wind speed of 220 km/h the structure behaves elastically.

5. Reliability Analysis

The reliability analysis consisted of calculating the probability of failure, p_f, using Equation (1) and the reliability index, β, estimated by Equation (2). In this study, a value of 3.2 was adopted for the target reliability index, β_{target}, which indicates the adopted minimum safety level for structural elements subjected to wind load combinations, as indicated by [23]. This value was used for comparison with the reliability indices determined from the different analyses performed here.

5.1. Limit State Functions

Three different limit state functions were considered for the reliability analysis. These limit state functions are according to the main failure cases reported in these structures, and they are: (a) column base flexure-compression and (b) base plate flexure. The limit state functions for these two cases were determined based on the limit states given in the ANSI/AISC 360-22 [20] steel design code and they are given in Equations (4) and (5).

$$G_1(X) = 1 - \frac{P_{nc}}{2 \cdot P_c} - \frac{M_{nc}}{M_c} \quad (5)$$

$$G_2(X) = M_{nbp} - M_{bp} \quad (6)$$

where P_{nc} and M_{nc} are the axial compressive and bending moment nominal resistances of the column, respectively; P_c is the load force due to self-weight of the billboard and M_c is the bending moment due to the wind load forces. In the case of the base plate, M_{nb} and M_{bp} are the bending moment nominal resistance and the bending moment due to wind loads, respectively. Equation (5) is non-linear and it needs SORM solutions for reliability analysis and Equation (6) is linear, therefore, it was solved using FORM solutions. Both reliability analyses were performed using the FERUM computer program [14].

5.2. Probabilistic Parameters

To perform the reliability analyses, three main probabilistic parameters are required from the random variables. Namely, the bias factor, λ, defined as the ratio of the mean value to its nominal one; the coefficient of variation, COV, defined as the ratio of the mean value to its standard deviation, and the probability distribution of the random variables. The probabilistic parameters of the random variables involved in the limit states functions of Equations (4)–(6) are given in Table 8.

Table 8. Probabilistic parameters of the random variables.

Random Variable	Bias Factor, λ	Coefficient of Variation, COV	Probability Distribution	Source
P_{nc}	1.411	0.177	Log-normal	Norton et al. [24]
M_{nc}	1.050	0.072	Log-normal	MacPhedran [25]
P_c	1.050	0.10	Normal	Naghavi and Tavakoli [26]
M_c, M_{bp}, T_{rod}	0.6, 0.8, 1.0	0.15, 0.20, 0.25, 0.30, 0.35, 0.40	Gumbel	Ellingwood and Tekie [23]
M_{nbp}	1.0	0.034	Log-normal	MacPhedran [25]

It is important to clarify that internal force random variables caused by wind forces (M_c and M_b) have a bias factor and coefficient of variation that can change according to the wind location characteristics. For this reason, for these probabilistic parameters, the values shown in Table 8 were chosen, and adopted using common intervals specified by [23]. In this manner, Figures 15 and 16 were obtained for the limit state functions previously defined in Section 4.1, which are valid in the intervals defined for bias factor and coefficient of variation. In summary, Figures 15 and 16 were bound by a wide range of probabilistic parameter values and wind speeds. In this way, they cover a large spectrum of wind location characteristics instead of only one.

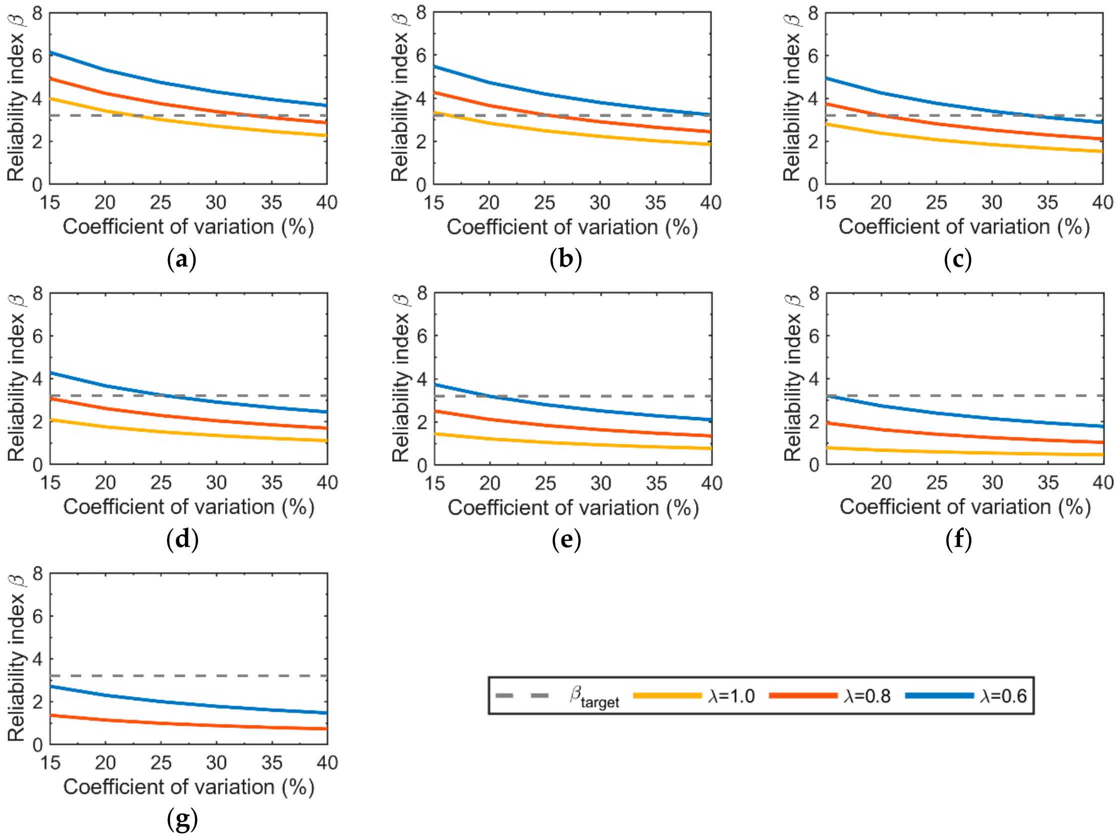

Figure 15. Reliability indices determined for the base column in flexure-compression. (**a**) V = 160 km/h; (**b**) V = 170 km/h; (**c**) V = 180 km/h; (**d**) V = 190 km/h; (**e**) V = 200 km/h; (**f**) V = 210 km/h; (**g**) V = 220 km/h.

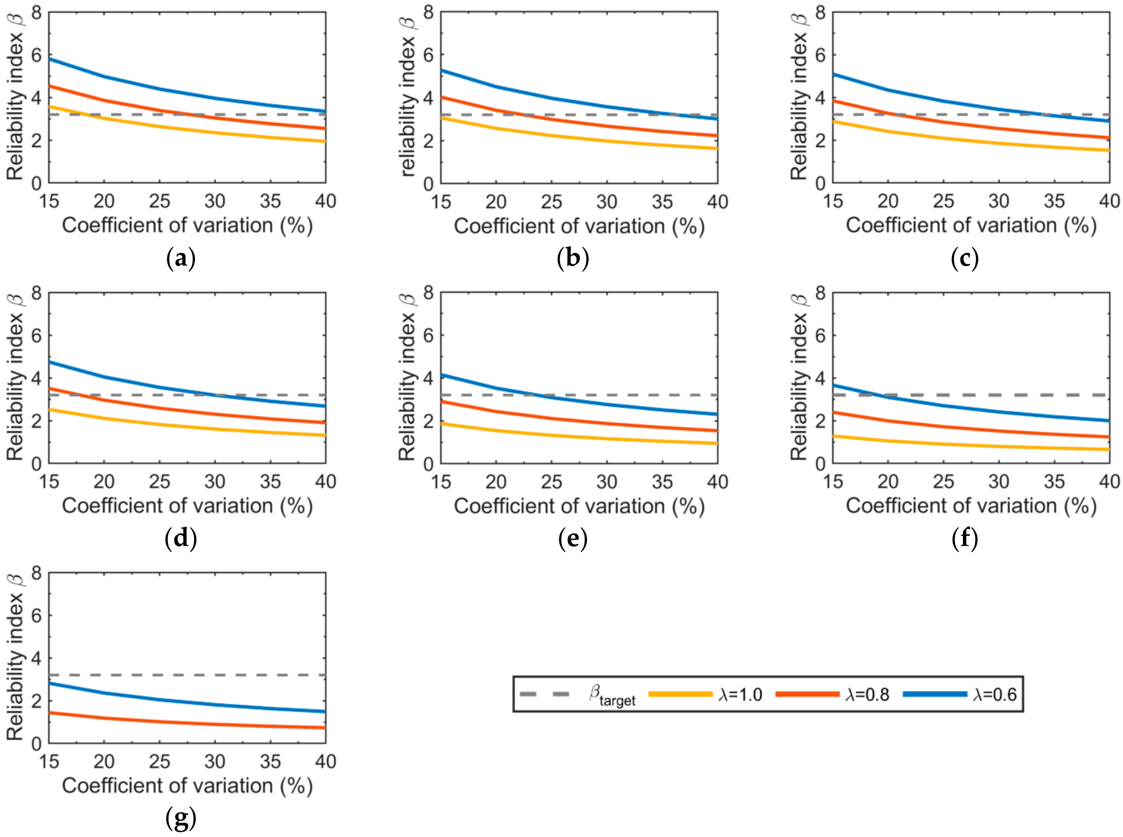

Figure 16. Reliability indices determined for the base plate in flexure. (**a**) V = 160 km/h; (**b**) V = 170 km/h; (**c**) V = 180 km/h; (**d**) V = 190 km/h; (**e**) V = 200 km/h; (**f**) V = 210 km/h; (**g**) V = 220 km/h.

5.3. Safety Levels

The reliability analysis results for the base column in flexure-compression and base plate in flexure are depicted in Figures 15 and 16. Safety levels determined for the base column in flexure-compression and base plate in flexure are very similar. From Figures 15 and 16, the target reliability index, β_{target}, of 3.2 was not reached, for any case of the probabilistic parameters, λ and COV, for wind speeds higher than or equal to 210 km/h (Figures 15f,g and 16f,g) and only for the lowest values of the involved probabilistic parameters for the wind speed of 200 km/h (Figures 15e and 16e). A Bias factor (λ) equal to 1.0 does not reach the β_{target} for all coefficient of variation (COV) values, for wind speeds equal to or higher than 170 km/h. It is important to analyze the case of wind speed of 180 km/h (Figures 15c and 16c) used as a reference for the wind design of the billboard with an exceedance probability of 0.02 (corresponding a return period of 50 years) according to [6]. In this case, β_{target} was achieved for COV values below or equal to 35% with a λ = 0.6 and only for COVs of 15% and 20% for λ = 0.8. Figures 15g and 16g do not show the curve for the case of λ = 1.0. Calculated reliability indices were all below zero, and higher than 50% probability of failure. In this range of values, the FERUM computer program cannot give reliable results; therefore, this curve was not shown in the previously mentioned Figures.

6. Conclusions

A methodology for determining the safety level of flexible single-post billboards is presented. Fluid and mechanical models were proposed and maximum values of internal forces and displacements in the most critical positions were obtained using linear elastic analysis. The maximum capacity of the billboard was determined by non-linear analysis and compared with those determined from the linear analysis. Limit state functions were determined according to the places most susceptible to damage. A reliability analysis was performed using the proposed probabilistic parameters of the random variables. Several wind speeds, bias factors and coefficients of variation were recommended. With the proposed methodology the following conclusions can be drawn:

1. Determined gust load factors (GLF) for all the evaluated reference wind speeds had values higher than 2.0 and with an increment rate of the wind speed. This indicates high dynamic interaction between wind and the billboard.
2. Modal analysis points out that the billboard has a similar first period in the directions parallel and perpendicular to the panel, resulting in 0.96 s and 0.95 s, respectively. This indicates a high flexible structure susceptible to wind dynamic interaction.
3. Negligible differences were noted between internal forces for head-on and north eastbound wind directions with higher values at 45° for all evaluated wind speeds. Therefore, reliability analyses were performed using the dominant wind direction.
4. The structural efficiency of the analyzed sections indicates that the column base and base plate were designed at their limits, while anchor rods were overdesigned. This was done due to uncertainties in the calculation of the tension force in anchor rods.
5. It was determined that the billboard behaves elastically for all evaluated wind speeds. However, high displacements were obtained, reaching 1250 mm for the reference wind speed of 220 km/h at 45° wind direction. Considering the dynamic effect caused by wind, large oscillations could happen, damaging elements attached to the panel or provoking structural elements to become loose.
6. Single post billboards cannot withstand more than 20 km/h of wind speed increment for any case of evaluated COV and λ values taken for the reference design wind speed of 180 km/h.
7. Wind codes could provide the fundamentals for performing CFD analysis in billboards prone to dynamic interaction with wind and to prove its accuracy. Furthermore, a methodology as presented here, should be provided to determine the safety level of billboards in places where there is uncertainty about the wind speeds and their probabilistic parameters.

To sum up, reliability analysis of flexible single-post billboards indicates that these structures are prone to having safety levels below what is considered as the minimum level if the bias factor and coefficient of variation are higher than that defined for codes.

Author Contributions: Conceptualization of the structural model, J.Y.M.-M. and A.G.; conceptualization of the fluid model, E.A.E.-H. and I.E.H.-D.; methodology, including reliability analysis, R.S.-E.; software analysis, E.A.E.-H.; formal analysis, R.S.-E. and E.A.E.-H.; writing—original draft preparation, R.S.-E. and F.C.; writing—review and editing, A.L.H.-M. and S.A.Z.C.; funding acquisition, J.Y.M.-M. and A.G. All authors have read and agreed to the published version of the manuscript.

Funding: The article processing charge (APC) was funded by Universidad de Guanajuato Campus Celaya-Salvatierra and Universidad de Guanajuato Campus Irapuato-Salamanca.

Institutional Review Board Statement: Not applicable.

Informed Consent Statement: Not applicable.

Data Availability Statement: Not available.

Acknowledgments: The authors would like to acknowledge the support given to this study by Melesio Jácome-García, Luis Bernando Nieves-García, Jorge Eduardo Villalpando-Hernández and Antonio de Jesús Colorado-Landa during the elaboration of their bachelor theses performed in Universidad Veracruzana. The authors acknowledge the financial support of Universidad de Guanajuato Campus Celaya-Salvatierra and Universidad de Guanajuato Campus Irapuato-Salamanca for the payment of the article processing charge (APC) for publication in open access.

Conflicts of Interest: The authors declare no conflict of interest. The funders had no role in the design of the study; in the collection, analyses, or interpretation of data; in the writing of the manuscript, or in the decision to publish the results.

References

1. Wang, D.; Chen, X.; Li, J.; Cheng, H. Wind Load Characteristics of Large Billboard Structures with Two-Plate and Three-Plate Configurations. *Wind Struct.* **2016**, *22*, 703–721. [CrossRef]
2. Wen, J.; Xie, Q. Field Investigation and Structural Analysis of Wind-Induced Collapse of Outdoor Single-Post Billboards. *Eng. Fail Anal.* **2020**, *117*, 104810. [CrossRef]
3. Warnitchai, P.; Sinthuwong, S.; Poemsantitham, K. Wind Tunnel Model Tests of Large Billboards. *Adv. Struct. Eng.* **2009**, *12*, 103–114. [CrossRef]
4. Li, Z.; Wang, D.; Chen, X.; Liang, S.; Li, J. Wind Load Effect of Single-Column-Supported Two-Plate Billboard Structures. *J. Wind. Eng. Ind. Aerodyn.* **2018**, *179*, 70–79. [CrossRef]
5. Civera, M.; Surace, C. Non-Destructive Techniques for the Condition and Structural Health Monitoring of Wind Turbines: A Literature Review of the Last 20 Years. *Sensors* **2022**, *22*, 1627. [CrossRef] [PubMed]
6. Certified Fraud Examiner, Idaho National Engineering and Environmental Laboratory. *Manual de Diseño de Obras Civiles, Cap. C.1.4 Diseño Por Viento*, CFE MDOC C.1.4, 2020th ed.; CFE: Mexico City, Mexico, 2020; ISBN 9798563923461.
7. *ASCE/SEI 7-10*; Minimum Design Loads for Buildings and Other Structures. American Society of Civil Engineers: Reston, VA, USA, 2013; ISBN 9780784412916.
8. *EN 1991-1-4*; Eurocode 1. Actions on Structures—General Actions—Wind Actions. British Standards Institution: Brussels, Belgium, 2010.
9. Letchford, C.W. Wind Loads on Rectangular Signboards and Hoardings. *J. Wind. Eng. Ind. Aerodyn.* **2001**, *89*, 135–151. [CrossRef]
10. Paulotto, C.; Ciampoli, M.; Augusti, G. Wind Tunnel Evaluation of Mean Wind Pressure on a Frame-Type Signboard. *J. Wind. Eng. Ind. Aerodyn.* **2006**, *94*, 397–413. [CrossRef]
11. Zuo, D.; Smith, D.A.; Mehta, K.C. Experimental Study of Wind Loading of Rectangular Sign Structures. *J. Wind. Eng. Ind. Aerodyn.* **2014**, *130*, 62–74. [CrossRef]
12. Aly, A.M.; Benson, J. Wind Loads on Overhead Sign Structures: A Comparative Study. *Appl. Sci.* **2023**, *13*, 1682. [CrossRef]
13. Hoang, B.A. Safety Evaluation of Billboards When Considering the Random Effects of Design Parameters in the Southern Region of Vietnam. In *Structural Health Monitoring and Engineering Structures*; Springer: Berlin/Heidelberg, Germany, 2021; Volume 148, pp. 313–329.
14. Haukaas, T.; Der Kiureghian, A. *Finite Element Reliability Using Matlab (FERUM). Computer Program for Reliability Analysis*; University of California: Berkley, CA, USA, 1999.
15. Zhang, Y.; Kiureghian, A. Two Improved Algorithms for Reliability Analysis. In *Reliability and Optimization of Structural Systems*; Springer: Boston, MA, USA, 1995; pp. 297–304.
16. Breitung, K. Asymptotic Approximations for Multinormal Integrals. *J. Eng. Mech.* **1984**, *110*, 357–366. [CrossRef]
17. Salgado-Estrada, R.; Zamora-Castro, S.A.; Herrera-May, A.L.; Sánchez-Moreno, Y.A.; Sánchez-Moreno, Y.S. Reliability Analysis of Prestressed Concrete Bridges in Mexico: Assessment and Live Load Factors Proposal. *Int. J. Civ. Eng.* **2021**, *19*, 481–499. [CrossRef]
18. ANSYS. *Documentation for ANSYS. ANSYS Workbench Release 16.2, 2016*; ANSYS: Canonsburg, PA, USA, 2016.
19. Ruiz Aguirre, D. Comportamiento de Conexiones Tipo Placa-Tope Bajo Carga Cíclica y Monótona Mediante Análisis de Elemento Finito. Master's Thesis, Universidad Nacional Autónoma de México, Ciudad de Mexico, Mexico, 2010.
20. American National Standards Institute; American Institute of Steel Construction. *Specification for Structural Steel Buildings*, 2022th ed.; AISC: Chicago, IL, USA, 2022.
21. Jung, C.; Schindler, D. The Role of the Power Law Exponent in Wind Energy Assessment: A Global Analysis. *Int. J. Energy Res.* **2021**, *45*, 8484–8496. [CrossRef]
22. Simiu, E.; Yeo, D. *Wind Effects on Structures*, 4th ed.; John Wiley & Sons, Ltd.: Chichester, UK, 2019; ISBN 9781119375890.
23. Ellingwood, B.R.; Tekie, P.B. Wind Load Statistics for Probability-Based Structural Design. *J. Struct. Eng.* **1999**, *125*, 453–463. [CrossRef]
24. Norton, T.R.; Mohseni, M.; Lashgari, M. Reliability Evaluation of Axially Loaded Steel Members Design Criteria in AASHTO LRFD Bridge Design Code. *Reliab. Eng. Syst. Saf.* **2013**, *116*, 1–7. [CrossRef]
25. MacPhedran, I.; Grondin, G.Y. A Simple Steel Beam Design CurveWork upon Which This Paper Is Based Was Presented at the 2008 CSCE Annual Conference in Quebec City on 11 June 2008. *Can. J. Civ. Eng.* **2011**, *38*, 141–153. [CrossRef]
26. Naghavi, F.; Tavakoli, H.R. Probabilistic Prediction of Failure in Columns of a Steel Structure under Progressive Collapse Using Response Surface and Artificial Neural Network Methods. *Iran. J. Sci. Technol. Trans. Civ. Eng.* **2022**, *46*, 801–817. [CrossRef]